# ENGINE AND LASER RESEARCHES OF A NOVEL INJECTOR WITH VARIED CROSS SECTION NOZZLE FOR PERFORMANCE INPROVEMENT

**Kazimierz Sowa, Marian Zabłocki**
*Krakow University of Technology*
*Institute of Automobile Vehicles and Internal Combustion Engines*
*ul. Warszawska 24, 31-155 Krakow, tel./fax: +48 12 628-20-47*
**Antoni Jankowski**
*Institute of Aeronautics, Al. Krakowska 110/114, 02-256 Warszawa,*
*tel +48 22 8460011, fax: +48 22 8464432, ajank@ilot.edu.pl*
**Aleksander Sandel**
*The National Automotive Center, Warren, MI 48397-5000, USA, sandela@tacom.army.mil*

***Abstract***

*Some results of preliminary engine performances and laser research are presented in the paper. Two kinds of injectors have been tested: the fist one – standard and the second – novel one on the basis of invention applied by M. Zablocki and J. Szymanski (P2944889). Investigations were conducted on the research Diesel engine equipped with varied cross section nozzle injector and on the LDV and PDPA laser equipment. The novel research prototype injector has needle, which executes rotational - reciprocal movement. The novel worked-out injector has outflow holes with flow section that executes a change during the injection process, which enables to decrease of diameter of fuel droplets. The measurements were performed at varied rpm (from 1000 rpm to 1600 rpm) and maximum fuel doses. The injector in relation to engine performance was not optimised. The objectives of the research were determination either the working quality of a novel injector and their influence on combustion process in different method of mixture preparation process. The obtained results show a direction of further researches that impact on system optimisation. Some results of novel injector concerning brake power, fuel consumption, CO emission and HC emission are the same or better than of standard injector. Other test results are not as good as expected. The reasons of worse test results have been investigated with the laser methods. One of them is leak of the prototype injector. After removing leakage, laser test results were much better.*

*Keywords: Diesel engine, fuel spray, variable orifice nozzle, engine performance, laser method, ecology*

## 1. Introduction

Standard Diesel injectors have hole nozzles of the same size. The hole size is a compromise between the specific requirements of power, fuel consumption, exhaust emissions, noise etc. Small hole sizes are good for low speed engine and low load. Large hole sizes are more suitable for high-speed engine and full loads. At low speeds and loads, the fuel spray from a standard sized nozzle does not produce proper mixture. The turbocharged boost pressure is low at the running conditions, which allows both the dense core of the spray and the fuel rich vapour phase to penetrate too far into the piston bowl, such that it is close to or on the walls. With a smaller hole diameter, the injection takes place over a longer period and with higher spray velocities, but the penetration into the cylinder is reduced. This results in improved mixing of the fuel and air and thereby lower smoke. Another benefit of a smaller final orifice is that less fuel is injected during the ignition delay period, which results in lower noise levels.

This forces the designers to give a new dimension to exhaust engine system together

with inlet system in order to improve exhaust gases contents just before they leave the cylinder. Among the systems, that are the parts of engine combustion system, a great role in generating fuel-air mixture plays the injection equipment, which, by influencing on fuel injection pressure, has an impact on intensity of mass flow rate from atomizer's nozzles, changes of range of atomised spray front and distribution of droplets in combustion chamber. In order to diminish concentration of above mentioned toxic exhaust elements high pressure of fuel injection is required. One of the reasons that causes the increase of particulate emission is occurrence in the initial and final stages of injection droplets of large diameters in fuel spray. In order to limit the occurrence of this effect large values of the injection pressure, reaching 200MPa, can be required. Another way of eliminating large fuel droplets can be also the injector with variable flow section at the beginning and at the end of fuel injection. Description of function and design of such injector with rotational - reciprocal needle movement is placed below.

## 2. Overview of the novel experimental prototype injector

View of the novel experimental prototype injector used in the researches is shown in the Fig. 1. Photograph of nozzles novel experimental injector with rotational - reciprocal movement of needle in the Fig. 2. Schematic design of novel experimental prototype injector with rotational - reciprocal movement of needle is shown in Fig. 3. Schematic design of upper part of novel prototype injector with rotational - reciprocal movement of needle is shown in the Fig. 4. The novel injector (P2944889 Polish patent applying) has variable cross-section of nozzle holes. It operates gradually revealing the cross-section of atomised nozzle holes at the initial and final stages of the injection process. Those changes of the cross-section of nozzles are caused by turning atomizer needle, which can perform rotational - reciprocal movement. The shape of injected spray does not have then compact, almost axial-symmetrical character, as it occurs in the standard injector. The spray is being extended in the vertical and horizontal plane due to discharge of the flow cross-section, which during opening and closing has lenticular shape. This shape is burden by the edges of atomizer hole (made in the needle) and outlet nozzles (made in the body of atomizer). Due to this fuel is being distributed in larger volume of the combustion chamber. More accurate design descriptions of such injector, which needle performs rotational - reciprocal movement can be found in other papers [5], [6], [7], [9]. The target of the novel injector is improvement of fuel spray preparation (fuel atomisation and spray penetration) and in this way – engine performance improvement, especially fuel consumption mainly at low engine speed and low loads, as well emissions and other engine performance.

## 3. Test bed for engine researches

Researches were carried out using single-cylinder direct injection Diesel engine water - cooled with forced circulation. The engine specifications are as follows:

- Bore – D = 127 mm,
- Stroke – S = 146 mm,
- Displacement – $V_s$ = 1.85 dcm$^3$,
- Compression ratio – $\varepsilon$=15.75,
- Rated engine speed – n = 2200 rpm,
- Type of injection pump – P56 (one section active only),
- Minimum engine speed – $n_{min}$ = 700 rpm,
- Type of injector – W1B with atomizer D1LMK 140/M2,
- Opening pressure of the needle value – $p_o$=17.0 MPa.

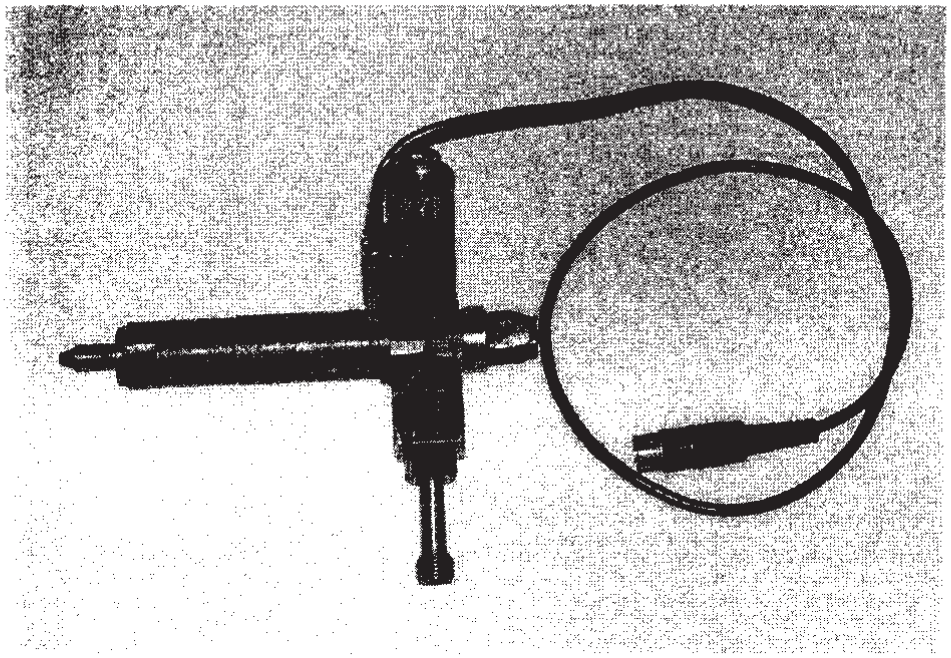

*Fig. 1. Photograph of the novel experimental prototype injector with rotational - reciprocal movement of needle*

Engine researches have been performed on the test bed comprising KS 37 A-4 electric brake, one cylinder research Diesel engine type SB 3.1, piezoelectric pressure transducer, piezoamplifier, injector (standard or novel with rotational - reciprocal movement of needle), inductive needle lift transducer, strain bridge, PC with plug-in card, indimeter, supply pump, injection pump, optical angle encoder, signal decoder, exhaust gas emissions system analysers, fuel tank, fuel meter, time meter, smoke meter. The layout is shown in the Fig. 5. Engine measurements aiming at determining of engine parameters defining indicators values characteristic for engine operations and fuel combustion processes were held at test bed. Researches had comparative character between 3-holes atomizer type of D1LMK 140/M2 (standard) and experimental one M with needle performing rotational - reciprocal movement.

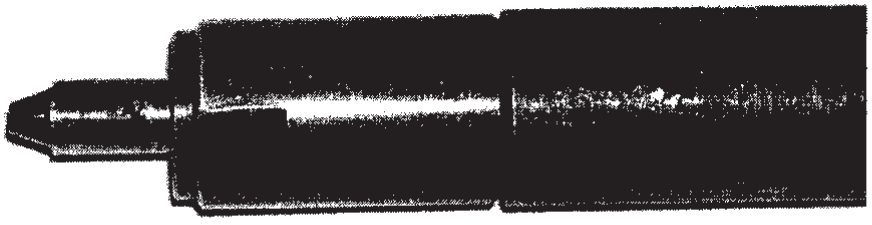

*Fig. 2. Photograph of nozzles novel experimental injector with rotational - reciprocal movement of needle*

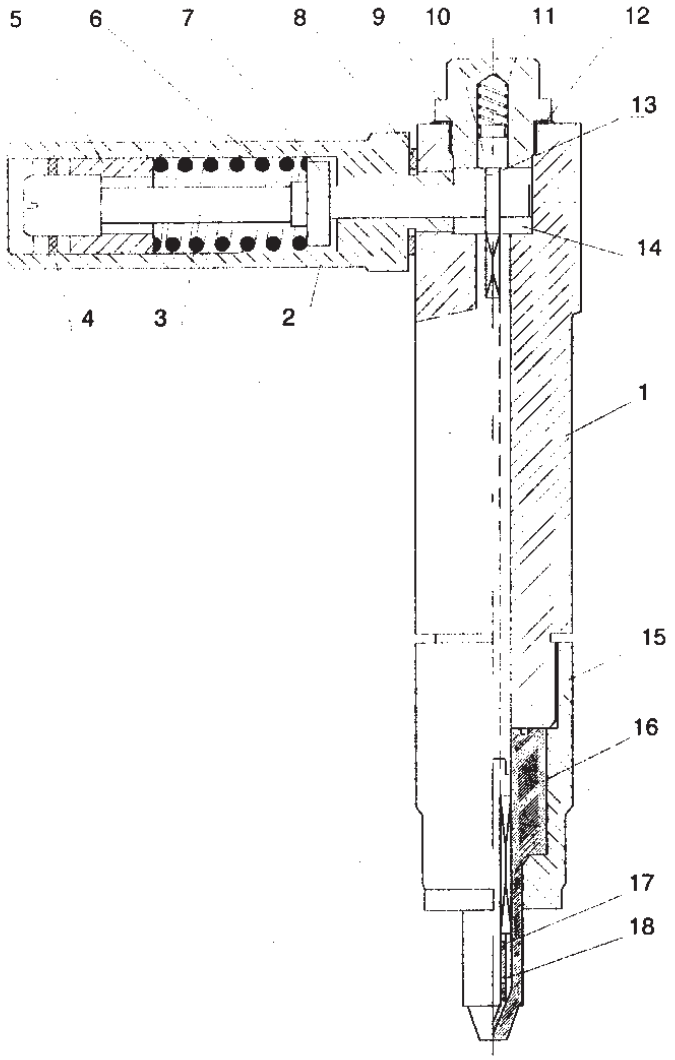


*Fig. 3. Schematic design of novel experimental prototype injector with rotational - reciprocal movement of needle 1 Holder body; 2 Booster; 3 Buffer; 4 Lock nut; 5 Adjusting screw; 6 Spring; 7 Plunger; 8 Washer; 9 Cup screw; 10 Compression piston; 11 Compression spring; 12 Washer; 13 Driver pin; 14 Needle driver; 15 Cup nut; 16 Nozzle body; 17 Needle; 18 Transversal hole*

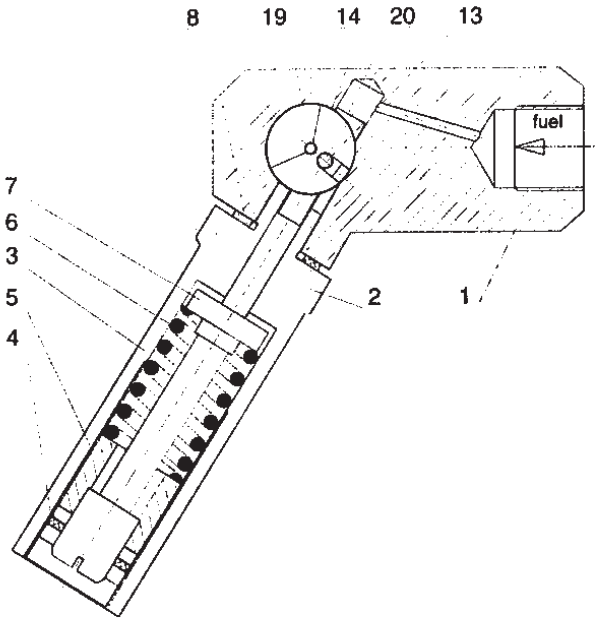


*Fig. 4. Schematic design of upper part of novel prototype injector with rotational - reciprocal movement of needle 1 Holder body; 2 Booster; 3 Buffer; 4 Lock nut; 5 Adjusting screw; 6 Spring; 7 Plunger; 8 Washer; 13 Driver pin; 14 Needle driver; 19 Hole in driver; 20 Piston active face*

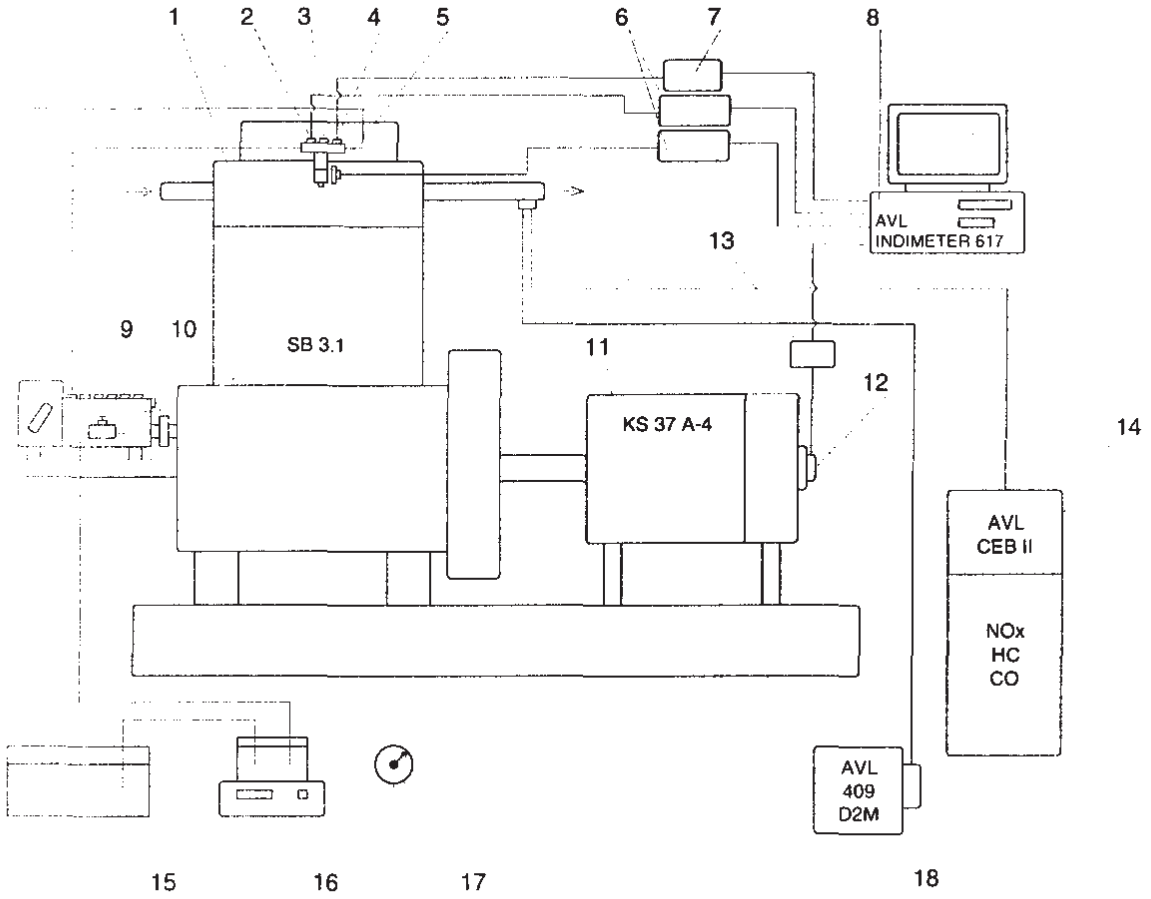


*Fig. 5. Schematic layout of engine test bed*

*1. Single-cylinder research Diesel engine type SB 3.1, 2. AVL 5QP6002 Piezoelectric pressure transducer, 3. Injector (standard or novel with rotational - reciprocal movement of needle), 4. Inductive needle lift transducer, 5. AVL 5QP6002 Piezoelectric pressure transducer, 6. AVL 3056 Piezoamplifier, 7. Strain bridge, 8. PC with plug-in card AVL Indimeter 617, 9. Supply pump, 10. P56-01 Injection pump, 11. KS 37 A-4 Electric brake, 12. AVL Optical angle encoder, 13. Signal decoder, 14. AVL CEBII Exhaust emissions system, 15. Fuel tank, 16. WT 1000 Fuel meter, 17. Time meter, 18. AVL 409 D2M Smoke meter*

## 4. Laser equipment

The Phase Doppler Method is based on the principles of light scattering interferometry. Measurements are made at a point referred to as the probe volume, which is determined by the intersection of two laser beams. As a particle passes through the probe volume, it scatters light from the interference fringe created by the intersecting laser beams. A receiving lens projects a portion of this refracted light onto several detectors. Each detector produces a Doppler burst signal. System uses a unique method to directly measure the sample volume simultaneously with particle size (PDPA) and velocity (LDV) and enables an accurate determination of the particle number density and volume flux. The Phase Doppler method requires no calibration because the particle size and velocity are depended only on the laser wavelength and optical configuration. PDPA measurements are not based on the scattered light intensity, and, consequently, are not subject to errors from beam attenuation or deflection which occur in dense particle and combustion environments. Block schema of LDV and PDPA Laser Equipment is shown in the Fig. 6. View of 3-Beam Spectra Physics Laser and Bragg Cell, which splits one beam on two, is shown in the Fig. 7. View of measurement space with injector tested, LDV, PDPA Transducers is shown in the Fig. 8. 3-LDV Analysers, PDPA Analyser, Traverse Programmer, Computer with Printer, Oscilloscope are shown in Fig. 9. Raw Doppler Burst Signal in Tektronix Oscilloscope Screen during measurement is shown in the Fig. 10.

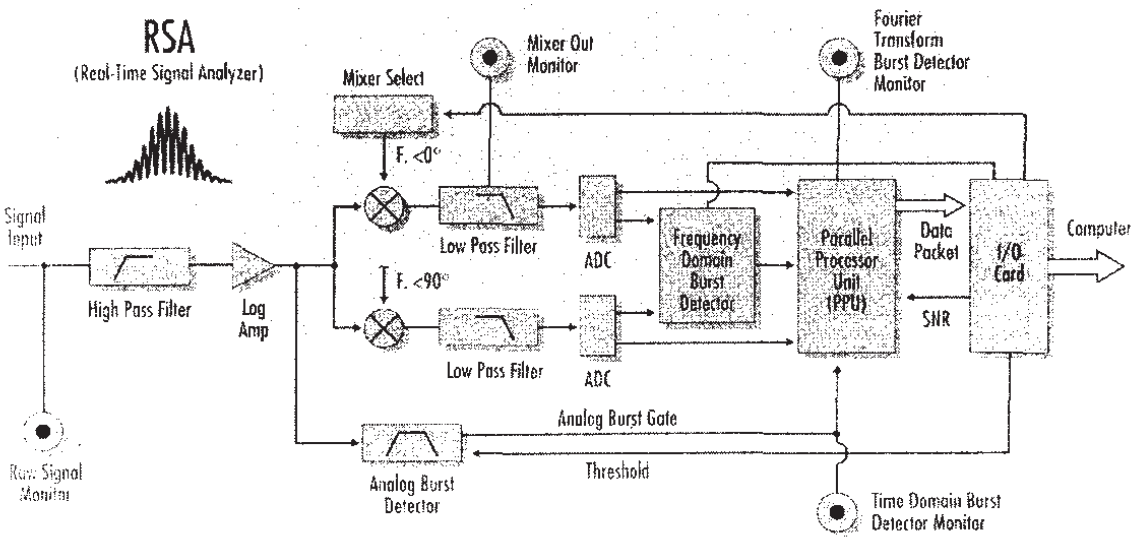


*Fig. 6. Block schema of LDV and PDPA Laser Equipment*

Investigation of fuel spray atomisation spectrum from both injectors has been carried out with use of dynamic laser analyser LDV (Laser Doppler Velocimeter) and PDPA (Phase Doppler Particle Analyser) made by Aerometrics. The Spectra Physics argon ion laser (5000 mW) has been used in the experiment. Measurement system enables realization of velocity measurements in 3 directions (3D).

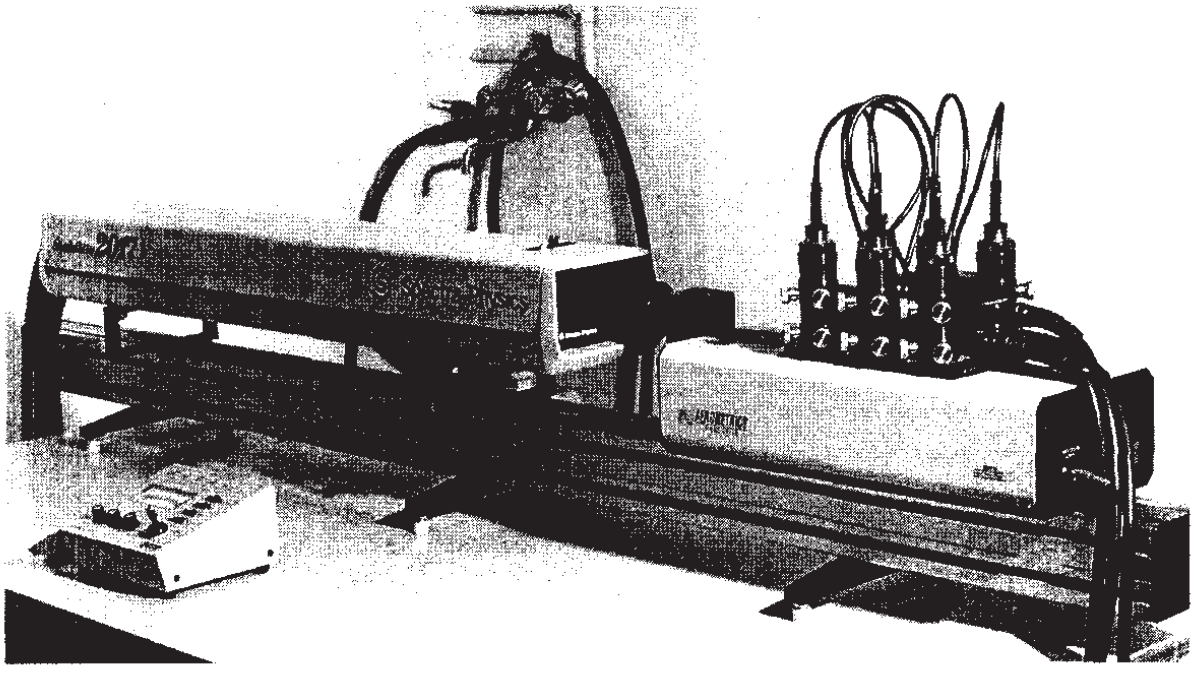

*Fig. 7. View of 3-Beam Spectra Physics Laser and Bragg Cell*

An interference pattern composed of light and dark fringes is formed at the point of intersection of the two beams. The distance between the fringes is known and is dependent only upon the angle of intersection $\phi$ and the frequency of the laser light $f_o$. Even the smallest droplets passing through the optically striped focal region cause the light is scattered in all directions.

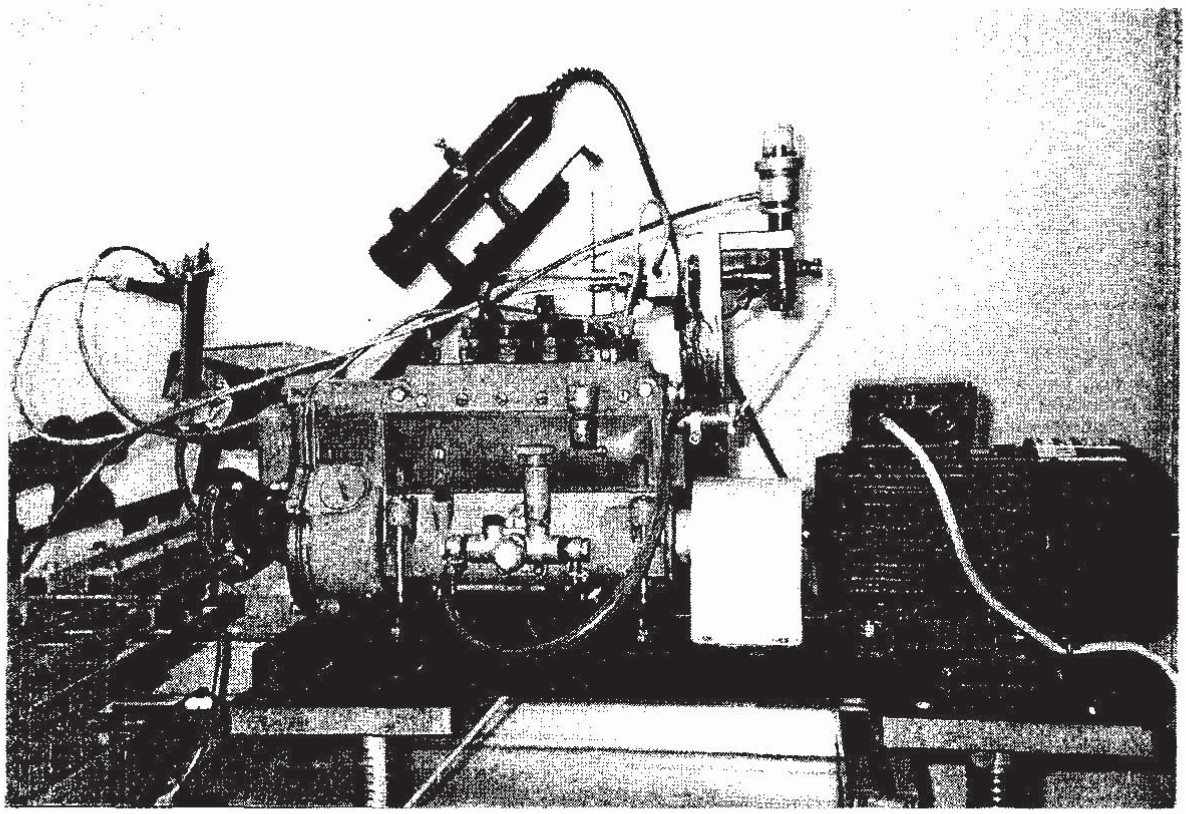

*Fig. 8. View of measurement space with injector tested, LDV, PDPA Transducers*

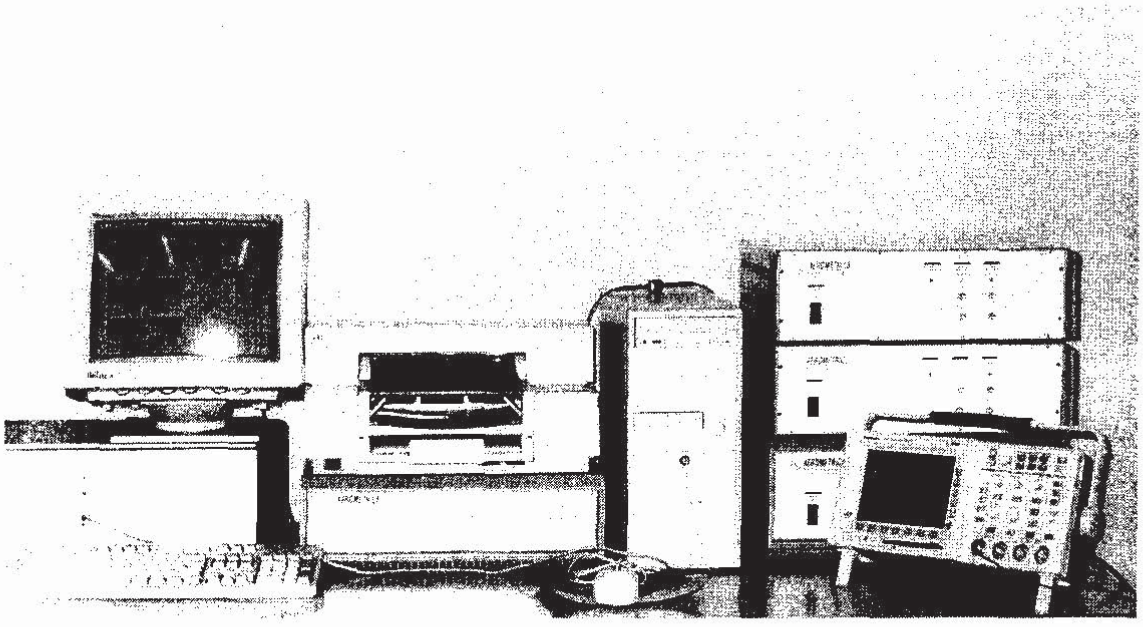

*Fig. 9. 3-LDV Analysers, PDPA Analyser, Traverse Programmer, Computer with Printer, Oscilloscope*

The front lens of the LDV collects the scattered light and directs it to the photo detectors (APD), which produces an electrical signal, proportional to the scattered light intensity. The intensity modulation $f_D$ of the scattered light, caused by the droplet passing vertically through the stripped measurement volume, is directly proportional to the droplet's velocity. The measurement principle of velocity component consists in registration of change in laser beam frequency, which is proportional to fuel droplet velocity. Droplet dimension measurements consist in registration of laser beam deviation while passing by the droplet, which is proportional to its diameter.

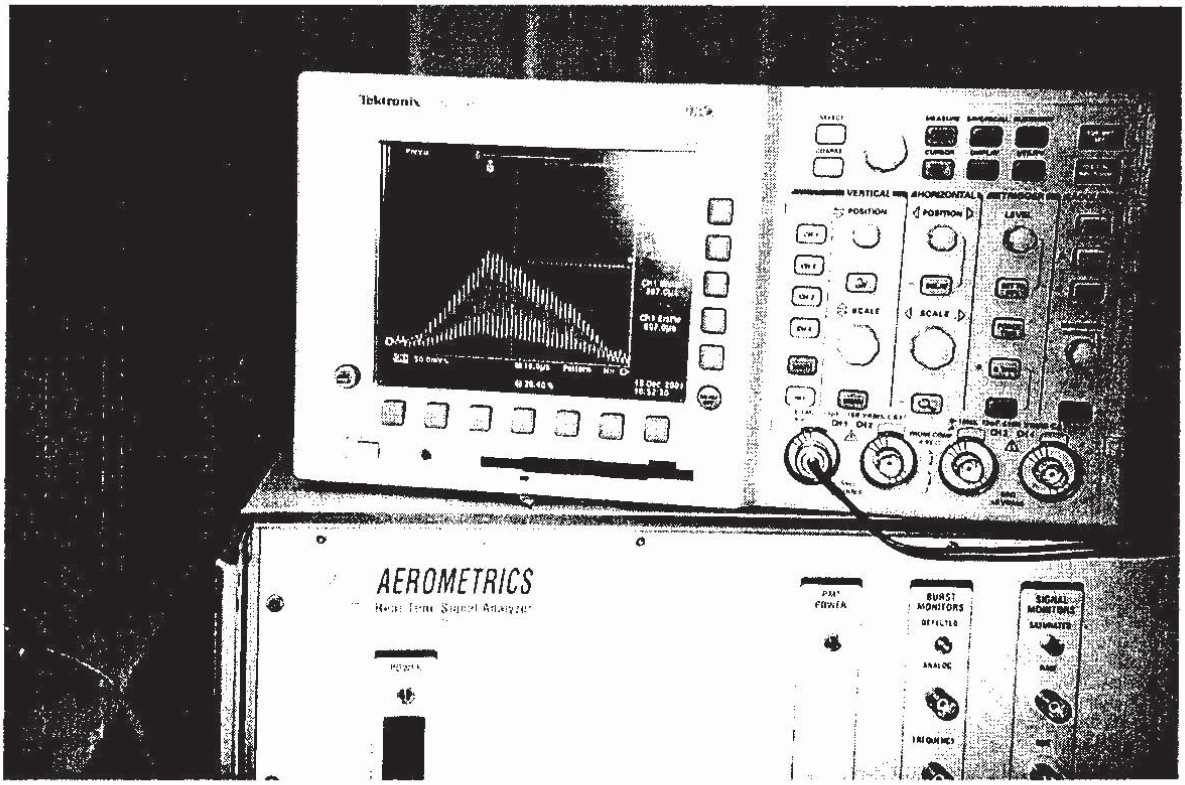


*Fig. 10. Raw Doppler Burst Signal in Tektronix Oscilloscope Screen*

Measurements are realized in the region, which is determined by two crossing laser beams, the zero one and Doppler one. The test section occurs in the field of optical focus of laser transmitter and has the shape of rhomboidal, whose maximal dimensions in the optical system amounted to 17.6 mm x 1.4 mm x 1.4 mm. The diameter of laser beam is 1.4 mm, distance between zero and Doppler beams amounted to 39.74 mm, and focal length is 250 mm. The measurements of test section can be altered with the use of the optical transmitter system, which should be matched with the anticipated range of droplets diameters occurring in the atomised fuel spray. Droplets diameters, which can be measured, range from 0.5 μm even till 3.822 mm. The best results can be obtained by using the optical system that matches atomised fuel spray, in which droplet diameter is 300 times bigger than the minimum one. Measurement range of diameter depends on optical system and type of RTSA (Real Time Signal Analyser) processor. Phase displacement of laser beam ranging from 3° to 350° can be registered. In all cases optical system should be set up, in a way that maximal droplets diameter is smaller than the shorter rhombus diagonal perpendicular to velocity component of fuel spray. Minimum droplets diameter, which can be registered, can amount to 0.5 μm or can cause phase displacement of laser beam by minimum 3°. Measurement system enables realization of velocity measurements in 3 directions (3D). The measurement principle of velocity component consists in registration of change in laser beam frequency, which is proportional to fuel droplet velocity. Velocity component can be determined by using the following formula:

$$v_i = \frac{f_D}{f_0 2 \sin \Phi}$$

where:

$v_i$ - droplet component velocity,
$f_D$ - modulated frequency of Doppler laser beam,
$f_0$ - laser light frequency,
$\Phi$ - angle of intersection laser and Doppler beams.

Measurement system allows utilization of 3 different laser beams: green one of 514.5 nm wavelength, blue one of 488 nm wavelength, and violet one of 476.5 nm wavelength. Droplet diameter measurement consists in registration of laser beam deviation while passing by the droplet, which is proportional to its diameter. Fuel droplet is observed from two detectors of two different distances: AB = 10.79 mm and AC = 32.15 mm. Each droplet is measured repeatedly and measurements results are compared. If the differences in measurements exceed 10%, the measurements results are rejected.

The computer records measurements results of each single droplet moving through rhomboidal test section. Measurement laser, together with Bragg Cell, which enables to obtain two beams (zero and Doppler ones) from one laser beam, alongside with six light pipe system, which allows performing tests in natural conditions

The measurement of droplet size and velocity is based on the observation of the light scattered by droplets passing through the crossover region of two intersecting laser beams. In practice, a single laser beam is split into two coherent beams of equal intensity and parallel polarization, which are made to cross. Droplets passing through the intersection of the two beams scatter light that produces information from which the droplet velocity v is calculated as

$$v = \frac{\lambda f_D}{2\sin(\Theta/2)}$$

where $\mu$ is the wavelength of laser light, $f_D$ the Doppler frequency, and $\Theta/2$ the laser beam intersection half-angle.

Size information is contained in the relative modulation visibility (V) of the scattered signal. The term visibility was defined by Michelson as

$$V = \frac{I_{max} - I_{min}}{I_{max} + I_{min}}$$

where $I_{max}$ and $I_{min}$ are maximum and minimum values of fringe-modulated signal.

## 5. Engine research results

Engine measurements were carried out in relatively narrow range of engine speed from 1000 to 1600 rpm, in order to avoid overload of prototype booster operator mechanism of injector, which guarantees rotational - reciprocal needle movement. Angle of the start of injection adjusted for both injectors amounted to $\Theta$=27° CA before TDC. Pressure, at which needle starts to raise (in standard injector) or piston in booster (in prototype injector) starts to move, amounted to $p_o$=17.0 MPa. The results of engine researches are shown in the Fig. 11 – 18, where circle solid symbols mark measurement points for standard injector (STD) and up triangle symbols mark measurement points for the novel experimental prototype injector with rotational - reciprocal movement of needle (INV). Solid lines mark relations (all: versus rpm) for standard injector and dash lines – relations for the novel experimental prototype injector with rotational - reciprocal movement of needle. All the relations have been obtained with 3-order polynomial fitting. The relations are as follows:

$$Y = A0 + A1\,X + A2\,X^2 + A3\,X^3,$$

where: A0, A1, A2, A3 are obtained from measurement points with least square method for the 3-order polynomial function and X represents engine speed [rpm]

Statistic relations for the measured performance parameters are:

**Torque (Y) versus rpm (X):**

STD: $Y_{T_S}$ =22+0.21365 X-1.39286E-4 $X^2$+2.77778E-8 $X^3$ [Nm]

INV: $Y_{T_I}$ =205.42857-0.24341 X+2.26786E-4 $X^2$-6.94444E-8 $X^3$ [Nm]

**Break Power (Y) versus rpm (X):**

STD: $Y_{P_S}$ =-11.89571+0.04258 X-2.35714E-5 $X^2$+5.97222E-9 $X^3$ [kW]

INV: $Y_{P_I}$ =-7.30357+0.01899 X+3.86905E-6 $X^2$-3.47222E-9 $X^3$ [kW]

**Fuel consumption (Y) versus rpm (X):**

STD: $Y_{FC_S}$ =22.09286-0.05102 X+4.29762E-5 $X^2$-1.11111E-8 $X^3$ [kg/h]

INV: $Y_{FC_I}$ =-19.13036+0.04797 X-3.49405E-5 $X^2$+9.02778E-9 $X^3$ [kg/h]

**Specific break fuel consumption (Y) versus rpm (X):**

STD: $Y_{SBFCS}$ =250.44071-0.03911 X+2.07857E-5 $X^2$-5.30693E-19 $X^3$ [g/kWh]

INV: $Y_{SBFCI}$ =183.42786+0.12411 X-1.38429E-4 $X^2$+5.97222E-8 $X^3$ [g/kWh]

**Carbon monoxide emission (Y) versus rpm (X):**

STD: $Y_{CO_S}$ =93781.2043-182.1443 X+0.12662 $X^2$-2.97622E-5 $X^3$ [ppm]

INV: $Y_{CO_I}$ =-41648.21786+103.75035 X-0.08264 $X^2$+2.18233E-5 $X^3$ [ppm]

**Hydrocarbons emission (Y) versus rpm (X):**

STD: $Y_{HC_S}$ =-1801.88571+5.59483 X-0.00517 $X^2$+1.52056E-6 $X^3$ [ppm]

INV: $Y_{HC_I}$ =716.86786-0.30506 X-5.29952E-4 $X^2$+2.93333E-7 $X^3$ [ppm]

**Nitrogen oxides emission (Y) versus rpm (X):**

STD: $Y_{NOx_S}$ =7646.18357-12.8197 X+0.0094 $X^2$-2.48583E-6 $X^3$ [ppm]

INV: $Y_{NOx_I}$ =1946.01786+0.97353 X-0.00191 $X^2$+7.40278E-7 $X^3$ [ppm]

**Smoke emission (Y) versus rpm (X):**

STD: $Y_{S_S}$ =0.89429+0.00826 X-8.71429E-6 $X^2$+3.05556E-9 $X^3$ [$^o$ B]

INV: $Y_{S_I}$ =-54.40286+0.13109 X-9.46548E-5 $X^2$+2.25E-8 $X^3$ [$^o$ B]

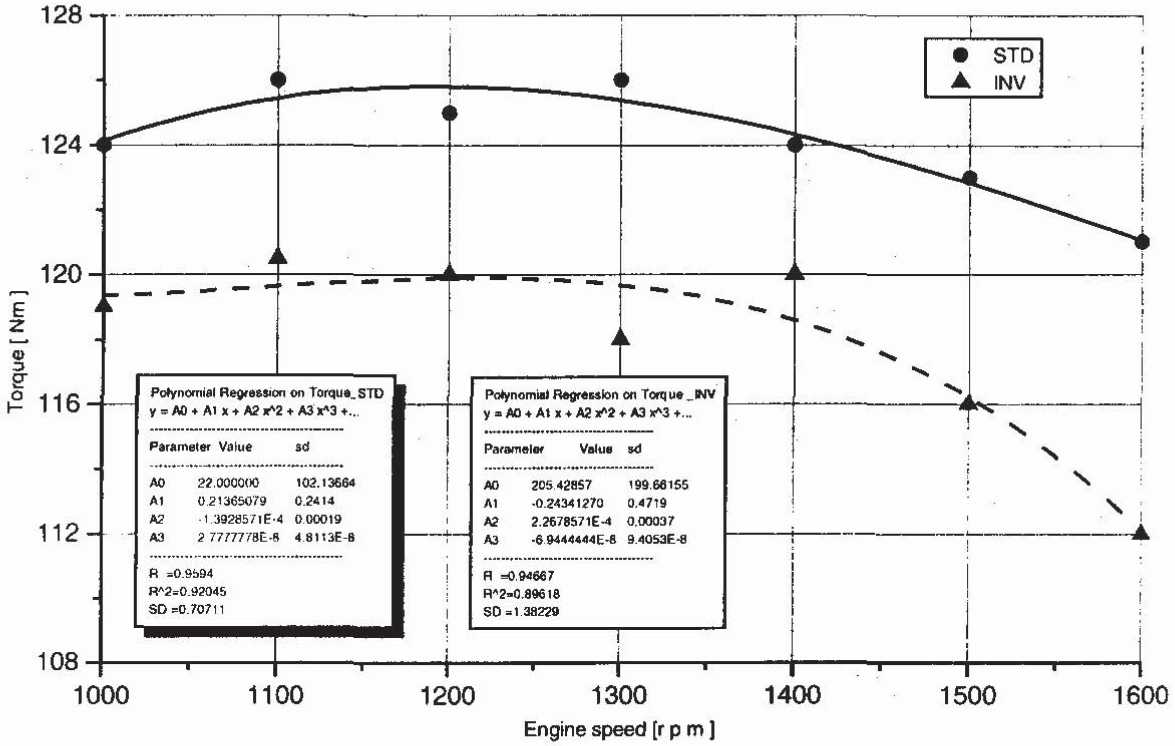


*Fig. 11. Torque versus engine speed for full load (solid line: standard injector, dash line: novel experimental prototype injector with rotational - reciprocal movement of needle) with 3 order polynomial regression (shadow frame: standard injector, black frame: novel experimental prototype injector with rotational - reciprocal movement of needle)*

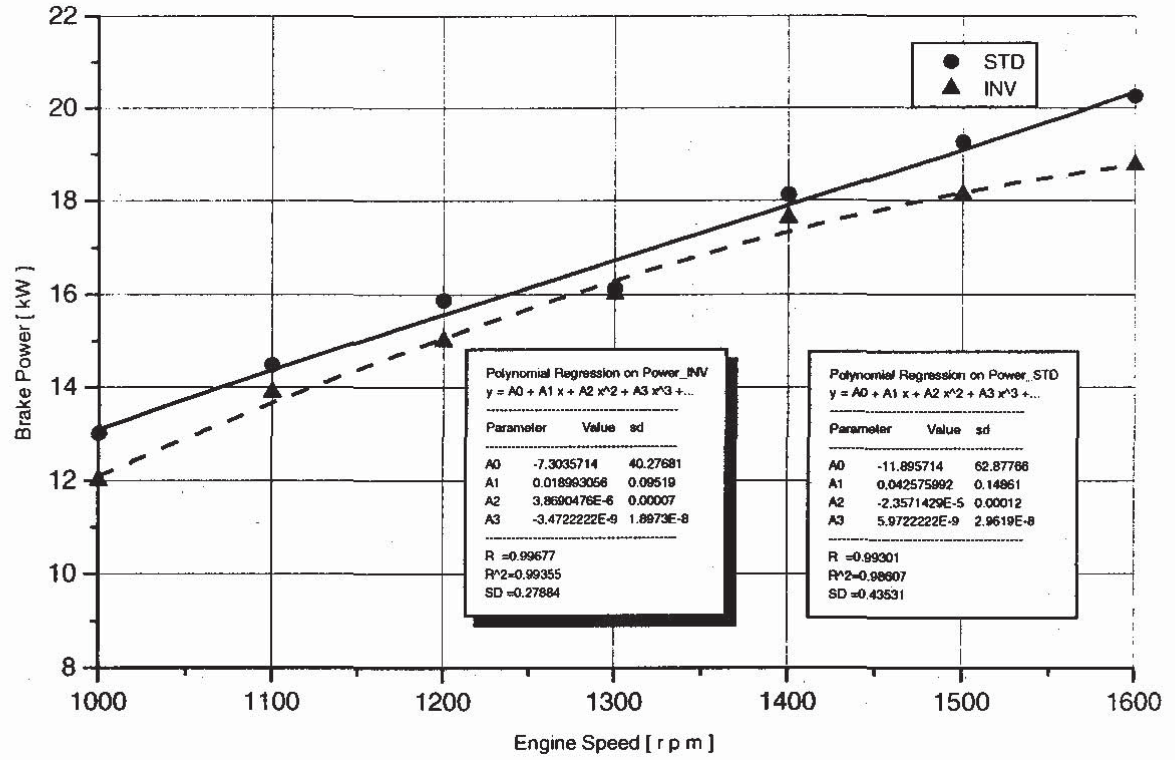


*Fig. 12. Break rated power versus engine speed for full load (solid line: standard injector, dash line: novel experimental prototype injector with rotational - reciprocal movement of needle) with 3-order polynomial regression (shadow frame: standard injector, black frame: novel experimental prototype injector with rotational - reciprocal movement of needle)*

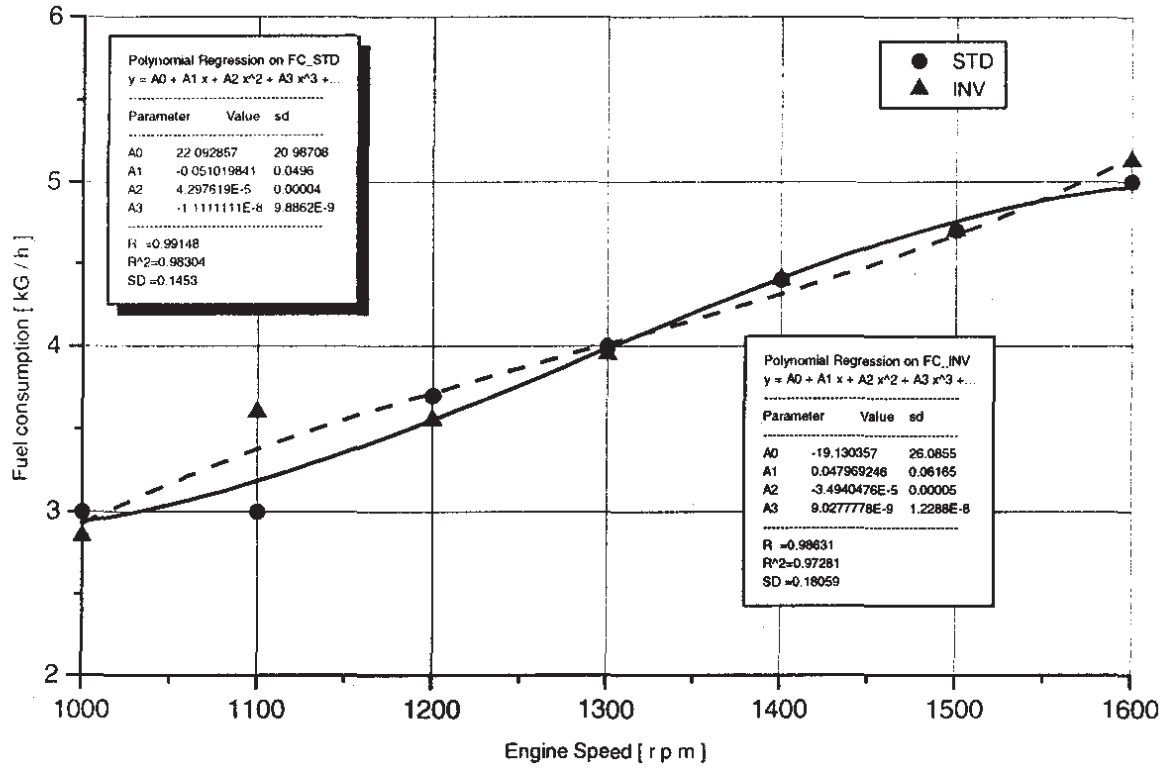


*Fig. 13. Fuel consumption versus engine speed for full load (solid line: standard injector, dash line: novel experimental prototype injector with rotational - reciprocal movement of needle) with 3 order polynomial regression (shadow frame: standard injector, black frame: novel experimental prototype injector with rotational - reciprocal movement of needle)*

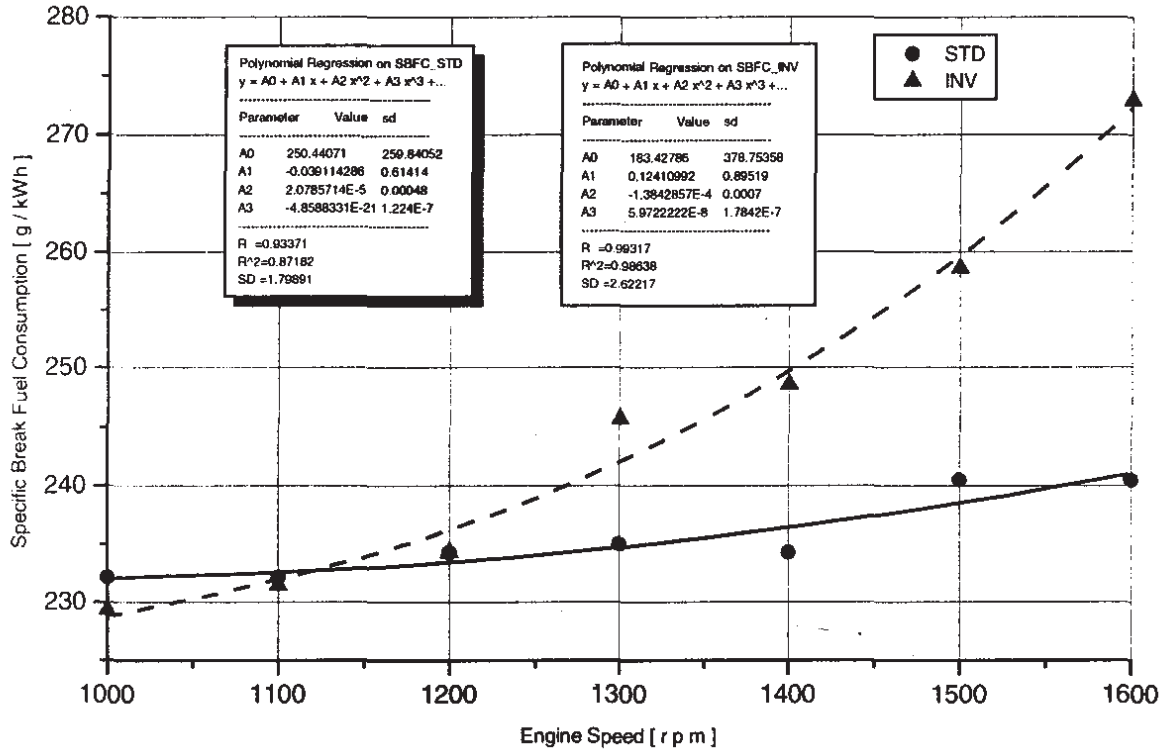


*Fig. 14. Break specific fuel consumption versus engine speed for full load (solid line: standard injector, dash line: novel experimental prototype injector with rotational - reciprocal movement of needle) with 3-order polynomial regression (shadow frame: standard injector, black frame: novel experimental prototype injector with rotational - reciprocal movement of needle)*

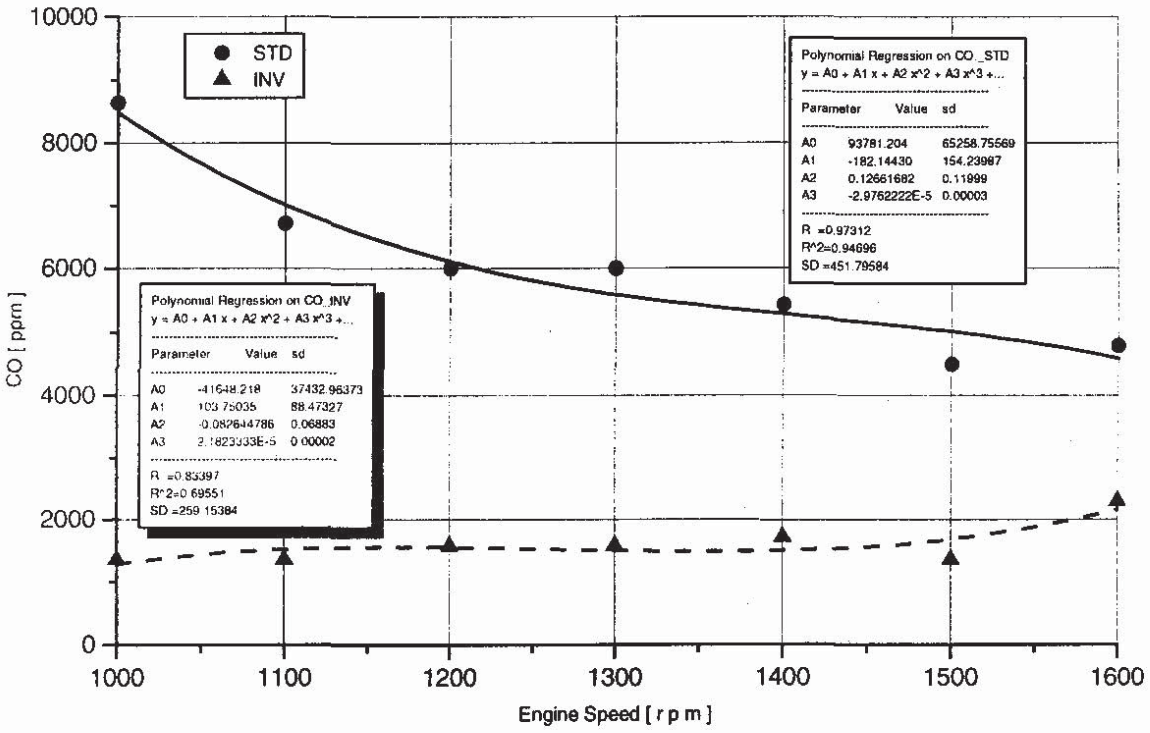


*Fig. 15. Carbon monoxide emission level versus engine speed for full load (solid line: standard injector, dash line: novel experimental prototype injector with rotational - reciprocal movement of needle) with 3 order polynomial regression (shadow frame: standard injector, black frame: novel experimental prototype injector with rotational - reciprocal movement of needle)*

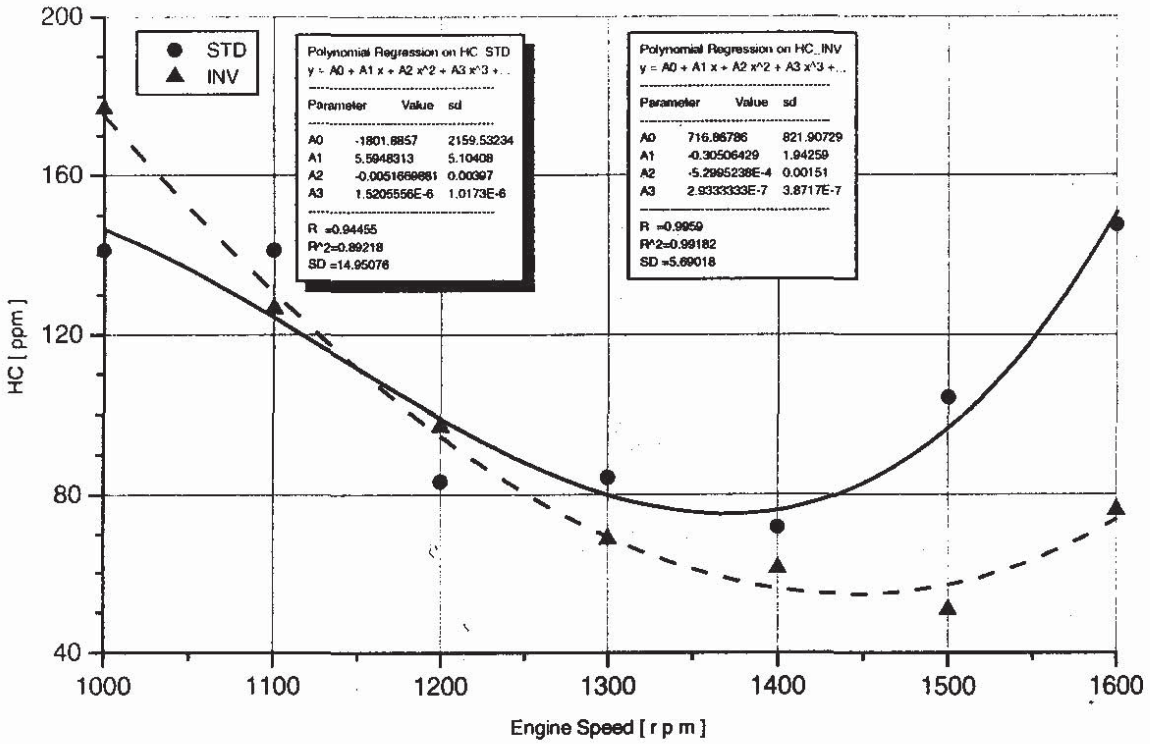


*Fig. 16. Hydrocarbons emission level versus engine speed for full load (solid line: standard injector, dash line: novel experimental prototype injector with rotational - reciprocal movement of needle) with 3 order polynomial regression (shadow frame: standard injector, black frame: novel experimental prototype injector with rotational - reciprocal movement of needle)*

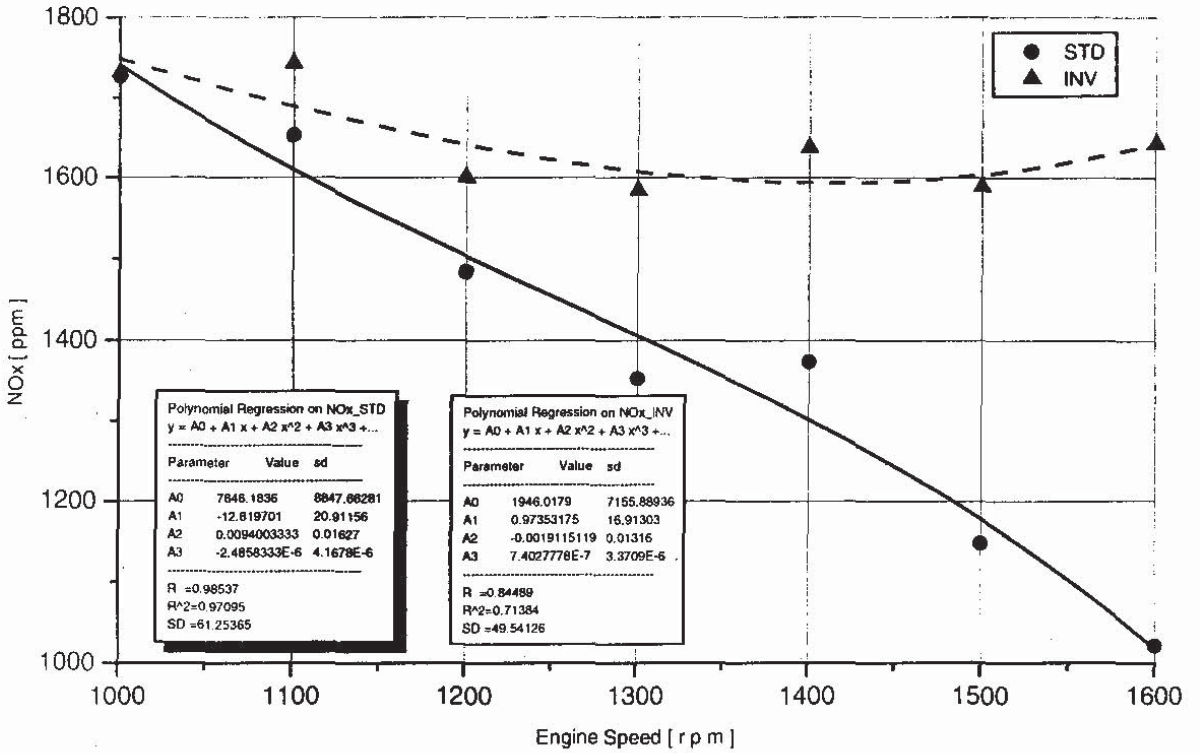


*Fig. 17. Nitrogen oxides emission level versus engine speed for full load (solid line: standard injector, dash line: novel experimental prototype injector with rotational - reciprocal movement of needle) with 3 order polynomial regression (shadow frame: standard injector, black frame: novel experimental prototype injector with rotational - reciprocal movement of needle)*

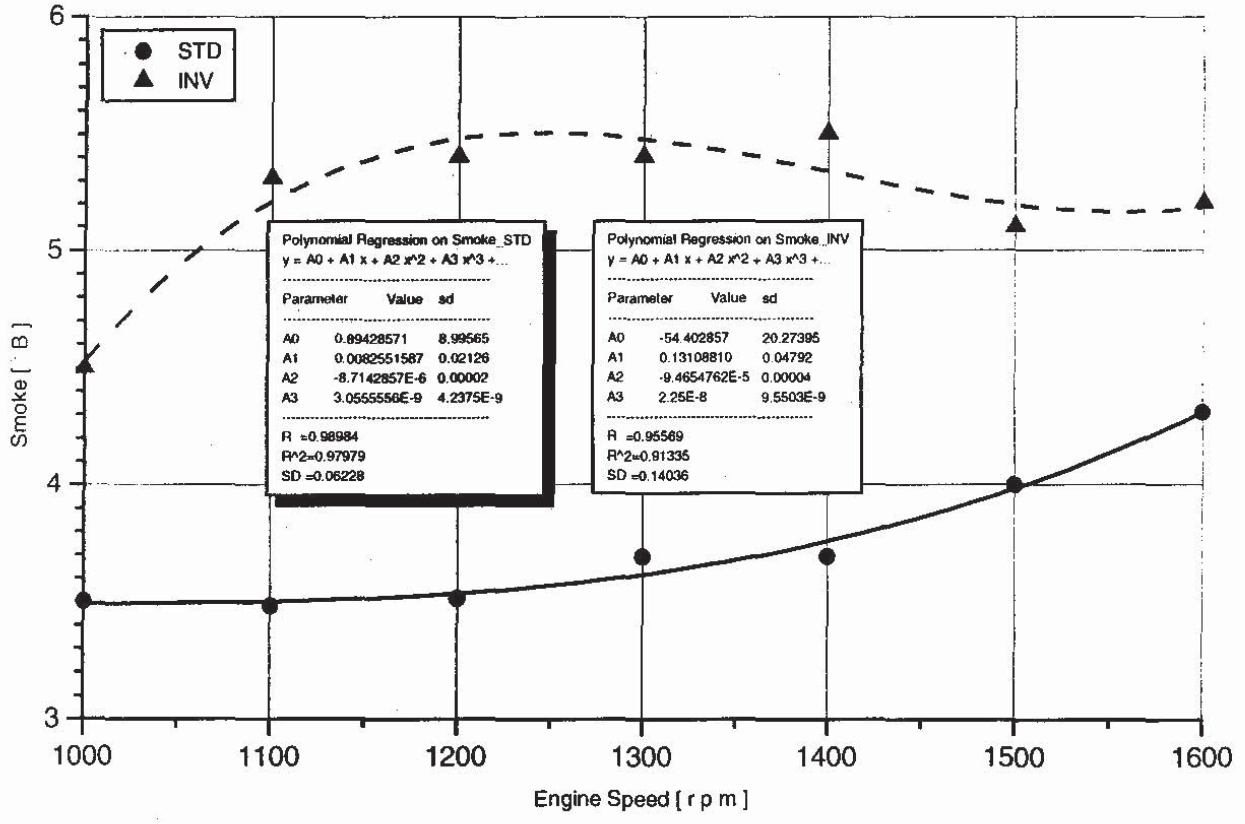


*Fig. 18. Smoke emission level versus engine speed for full load (solid line: standard injector, dash line: novel experimental prototype injector with rotational - reciprocal movement of needle) with 3-order polynomial regression (shadow frame: standard injector, black frame: novel experimental prototype injector with rotational - reciprocal movement of needle)*

Some more data concerning statistics are included in the Fig. 11 – 18 and concern values of standard deviation: sd for values A0, A1, A2, A3; SD for graphs; R for fitting of graphs. As the R is the closer to 1, as the graph fitting is the better.

As it results from Fig. 13, fuel consumption change curves $G_p$ have similar course and the differences occurring remain within the margin of error (around 1.5%). The use of prototype injector caused that in the examined range of engine speed, power output of engine $N_e$ and torque $M_o$ take smaller values from 4% till around 7.4%. This change is probably the result of influence of geometrical angle at the start of injection that was not optimised and equal for both injectors.

Fig. 14. shows a plot of specific brake fuel consumption as a function of engine speed. The curves indicate that specific brake fuel consumption for the tested engine with the novel injector is higher than with the standard one. Fig. 15. shows a dependence between carbon monoxide emission level and engine speed. The CO emission for engine with the standard injector is higher than for the engine with the novel one at all research engine speed range. Fig. 16 shows a dependence between hydrocarbons emission level and engine speed. The HC emission level for the engine with the novel injector is smaller at low engine speed and higher at bigger engine speed than for he engine with the standard one. Fig. 17. shows a plot of nitrogen oxides as a function of engine speed. The NOx emission level for the engine with the standard injector is smaller than for the engine with the novel injector at all the range of engine speed. Fig. 18 shows a plot of smoke as a function of engine speed. Smoke of exhaust gases for the engine with the standard injector is smaller than for the engine with the novel one.

For the prototype injector the geometrical angle at the start of injection value should be probably larger (around 30° CA before TDC) because needle performs idle rotary movement before the fuel outflow starts. The level of smoke of exhaust gases also takes larger values than these of standard injector. The reason for this probably lies in fuel post injection, which occurs at higher engine speed. Exhaust gas temperature (its changes are not shown in the photograph) is higher for the novel injector, which can be the result of not optimised angle of start of injection. Significant rise in specific fuel consumption, especially at higher engine speed, can be also the result of angle of start of injection, but also of increasing of combustion time. Analysis of heat release course during combustion process (these measurements were not placed in the paper) shows that for the prototype injector after self-ignition violent raise of heat release rate occurs connected with higher self-ignition delay. Instead, the second stage of combustion process (diffusion stage) is slower and probably lasts longer mainly due to fuel post injection which causes reduction in engine economy and higher temperature and exhaust gases smoke (Fig. 18).

Violent combustion in the first stage can be connected with higher emission of nitric oxides. On the other hand the novel injector proved significant reduction of CO and also, at higher engine speed, hydrocarbons HC. This may be associated with better fuel distribution in combustion chamber if using of novel injector.

It has to be underlined that presented measurements results were obtained without trade off not only the start of fuel injection, but also other design parameters of prototype injector, such as: pressure of start of needle movement $p_o$, spring rate B, diameters of atomizer orifices $d_o$.

Comparative regular injector was optimised considering the existing engine combustion system. The measurements results obtained show that it is necessary to perform optimisation of prototype injector. It is especially connected with eliminating fuel post injection. Under mechanical circumstance the prototype injector, with variable outlet cross-section nozzles, has worked correct.

## 6. Results of laser researches

Laser equipment has been applied for measurement velocity components and size of fuel droplets for two kind of injectors. The knowledge concerning diameter of droplets and their distribution in fuel spray is very important from point of view fuel consumption and emission. In general industrial flows and flows in injection process are turbulent. Turbulent motion is 3D, vertical, and diffusive, governing general Navier - Stokes equations which are very hard (or impossible) to solve:

$$\rho \frac{DU_i}{Dt} = \frac{\partial \tau_{ij}}{\partial X_j} + \rho f_i - \frac{\partial p}{\partial X_j}$$

There are few representative characteristics of mean droplet diameter used in the experiment descriptions. They include, among others, such means as arithmetic diameter (D10), surface diameter (D20), volume diameter (D30), Sauter diameter (D32), and Herdan diameter (D34).

With reference to PDPA system, five mean diameters were distinguished in order to determine spray parameters: D10, D20, D30, D32 and D43.

D10 diameter is known as arithmetic mean and its meaning is to make comparisons.

D20 diameter is described as droplet surface function, which enables to compare the average surface of measured droplets.

D30 diameter is droplet volume function which enables to compare the volumes of measured droplets.

D32 diameter (Sauter mean diameter) is derived from ratio of all droplet volumes sum to all droplet surface sum, and is used to analyse the processes of heat and mass exchange.

D43 diameter (Herdan diameter) is derived from ratio of the sum of the fourth power of droplet diameters to the sum of the third power of droplet diameters, and is used to analyse combustion processes, and gives a possibility of a closer examination of activities, which embrace combustion processes.

In Fig. 19 – 27 the results of laser measurement are shown. The results concerning velocities of fuel droplets are shown in the Fig. 19, 22 and 25 (velocity components of droplets – parallel and perpendicular to injector axis). The results concerning mean (D10, D20, D30, D32, D43) diameters of the fuel droplets are presented in the Fig. 20, 23 and 26. The results of diameter and volume distributions are presented in the Fig. 21, 24 and 27. Fig. 19 – 21 contain data for standard injector. Fig. 22 – 24 contain data for novel experimental prototype injector with rotational - reciprocal movement of needle. Fig. 25 – 27 contain data for novel experimental prototype injector with rotational - reciprocal movement of needle after improvement.

The results of diameter and volume of droplets distribution are matched by Rosin-Rammler function. This function for droplets size distribution may be expressed in the form:

$$1 - Q = \exp - (D/X)^q$$

but for the volume distribution is given by:

$$\frac{dQ}{dD} = q\,\frac{(\ln D)^{q-1}}{D(\ln X)^{q}}\,\exp-\left[\frac{\ln D}{\ln x}\right]^{q}$$

The Q is the fraction of the total volume contained in droplets of diameter less than D, and X and q are constants. By applying the Rosin-Rammler equations to spray it is possible to describe the droplet size distribution in terms of two parameters X and q. The exponent q is a measure of the spread of droplet sizes. If the q value is higher the spray is more uniform. The value of q in Rosin-Rammler function for most sprays is from 1.5 to 4.0.

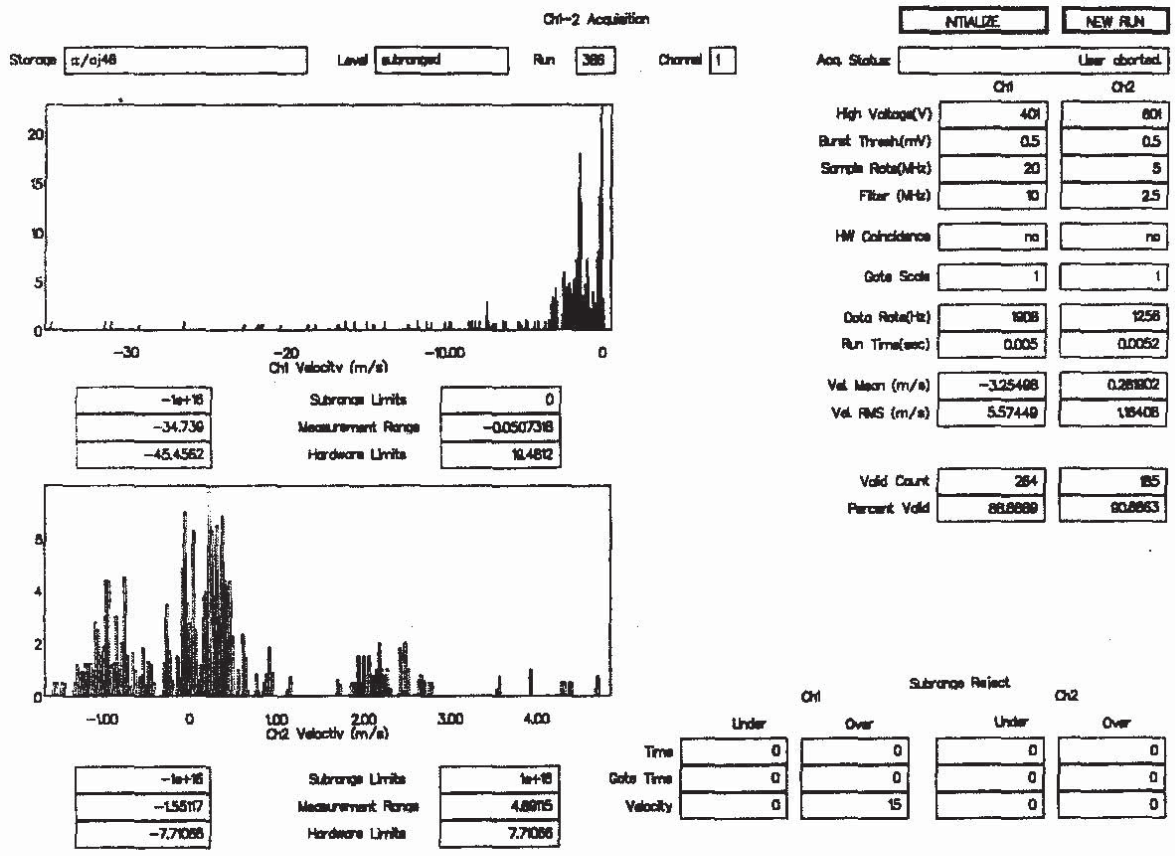


*Fig. 19. Velocity components of droplets for standard injector (Ch1 and Ch2 – parallel and perpendicular to injector axis as appropriate)*

Preliminary laser measurements show that for the same velocity components (Fig. 19 and 29) mean sizes of fuel droplets mean sizes for standard injector are fewer than for novel experimental prototype injector with rotational - reciprocal movement of needle as appropriate: D32 = 15.5 and 22.09 μm; D43 = 17.77 and 27.71 μm and after removing negative effects during closing D32 = 13.54 μm; D43 = 16.5 μm.

Size distribution for standard injector is described by equation:

$$1 - Q = \exp\,-(D/18.1986\quad)^{3.82203}$$

Volume distribution for standard injector is described by equation:

$$\frac{dQ}{dD} = q \frac{(\ln D)^{2.82203}}{58.52\ D} \exp - \left[\frac{\ln D}{2.9}\right]^{3.82203}$$

Size distribution for novel experimental prototype injector with rotational - reciprocal movement of needle is described by equation:

$$1 - Q = \exp - (D/25.3031)^{2.13982}$$

Volume distribution for novel experimental prototype injector with rotational - reciprocal movement of needle is described by equation:

$$\frac{dQ}{dD} = q \frac{(\ln D)^{1.12982}}{12.29\ D} \exp - \left[\frac{\ln D}{3.23}\right]^{2.12982}$$

Size distribution for novel experimental prototype injector with rotational - reciprocal movement of needle is described by equation after improvement:

$$1 - Q = \exp - (D/15.81)^{3.07931}$$

Volume distribution for novel experimental prototype injector with rotational - reciprocal movement of needle is described by equation after improvement:

$$\frac{dQ}{dD} = q \frac{(\ln D)^{2.07931}}{22.78\ D} \exp - \left[\frac{\ln D}{2.76}\right]^{3.07931}$$

Some cumulative results from laser measurements with the LDV and PDPA methods are in Tab. 1, where in the first row there are data for standard injector (STD), in the second row – data for novel experimental prototype injector with rotational - reciprocal movement of needle (INV) and in the last row – data for novel experimental prototype injector with rotational - reciprocal movement of needle after improvement (INV R). X represents computational values of mean diameters and q is an index exponent for size and volume distribution described by Rosin – Rammler equations. Examples of test results show that spray parameters for novel injector are worse than for standard one and that it is possible improving those parameters both by improvement manufacturing and by changes in orifice shape of the novel injector, especially for removing large droplets, which have influence on engine performance and which .were disclosed during laser tests.

Table 1. Cumulative data of laser measurements

| Injector | D32 | D43 | X | q | $V_m$ |
|---|---|---|---|---|---|
| | μm | μm | μm | | m/s |
| STD | 15.5 | 17.77 | 18.1986 | 3.82202 | 3.25 |
| INV | 22.09 | 27.71 | 25.3031 | 2.13982 | 3.22 |
| INV R | 13.54 | 16.5 | 15.81 | 3.07931 | 3.25 |

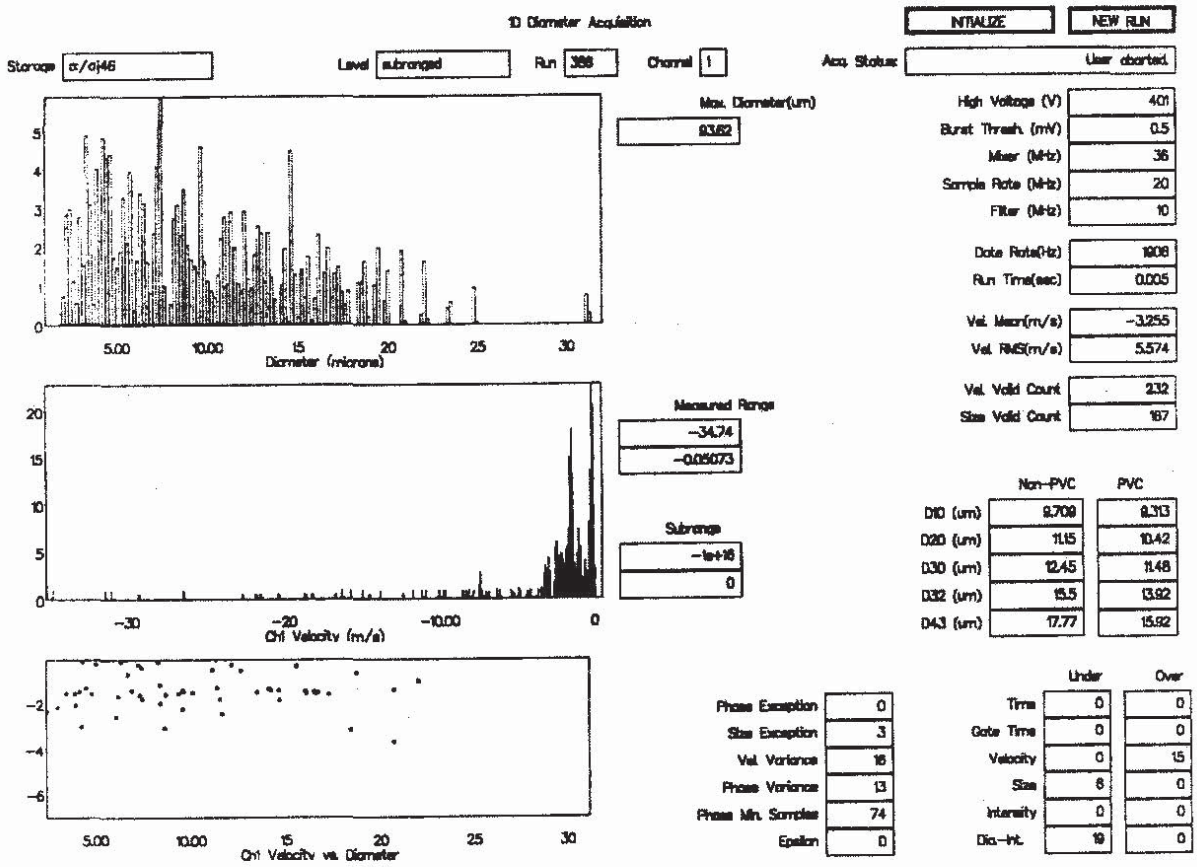


*Fig. 20. Mean diameters (D10, D20, D30, D32, D43) of droplets for standard injector*

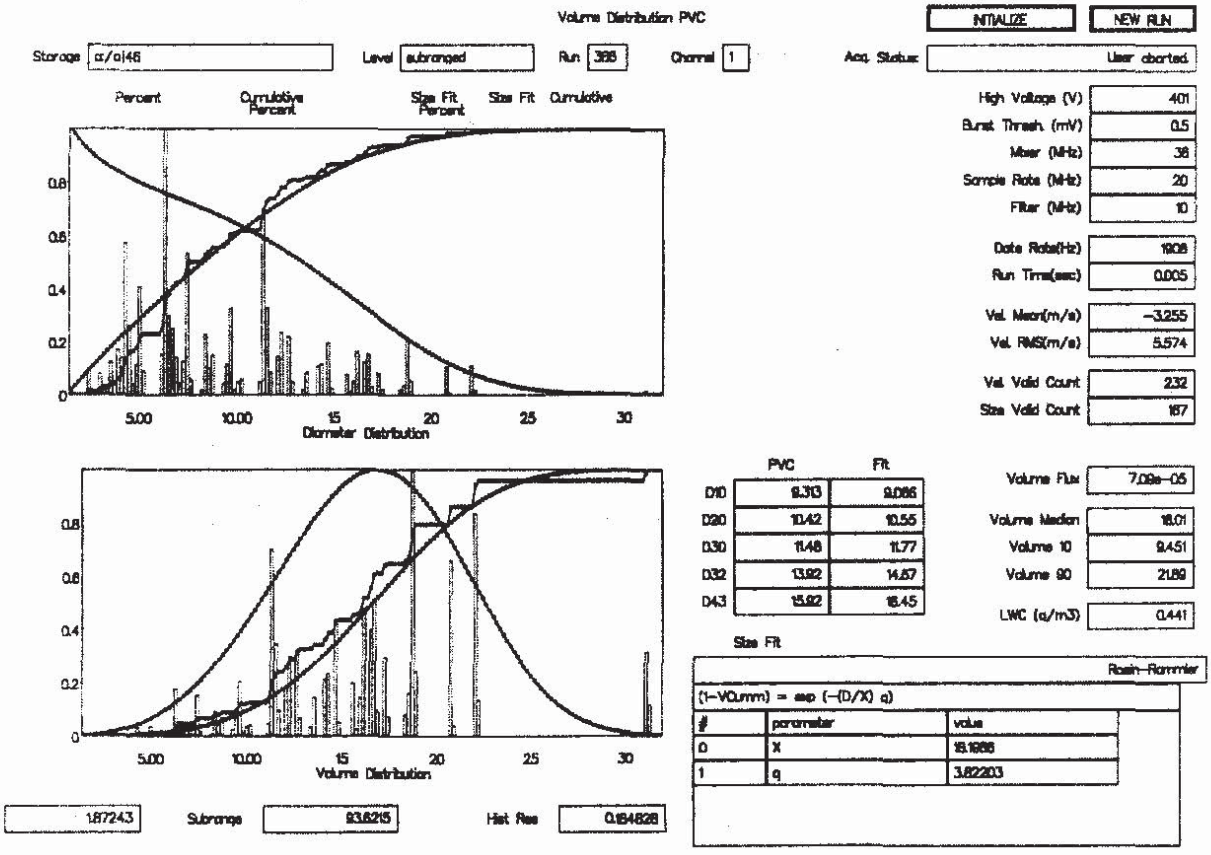


*Fig. 21. Cumulative size and volume distributions of droplets for standard injector*

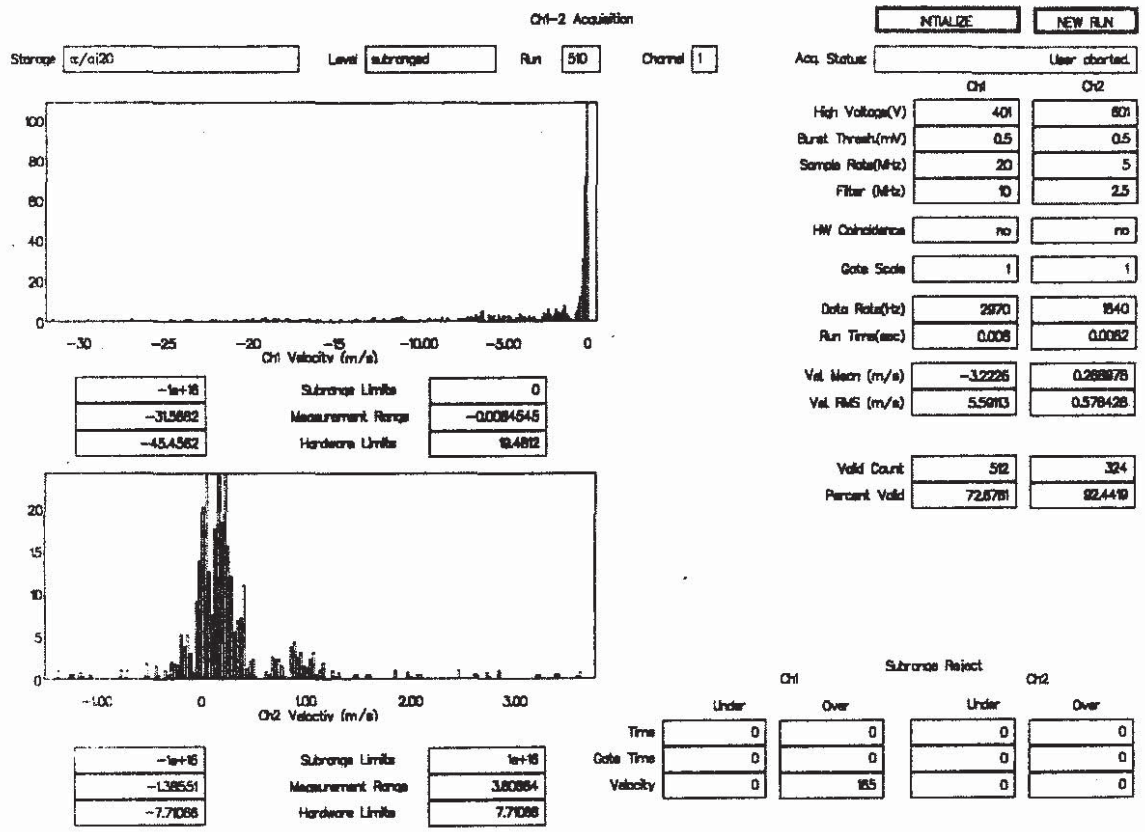


*Fig. 22. Velocity components of droplets for novel experimental prototype injector with rotational - reciprocal movement of needle (Ch1 and Ch2 – parallel and perpendicular to injector axis as appropriate)*

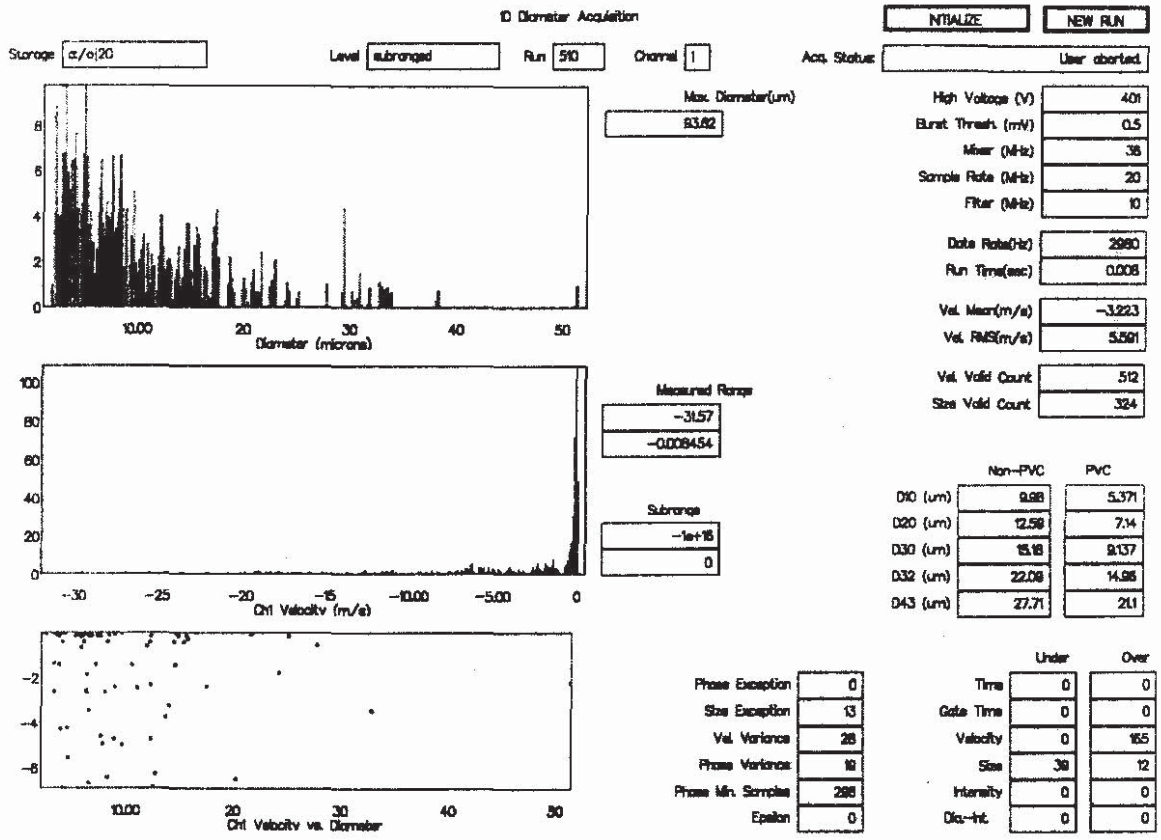


*Fig. 23. Mean diameters (D10, D20, D30, D32, D43) of droplets for novel experimental prototype injector with rotational - reciprocal movement of needle*

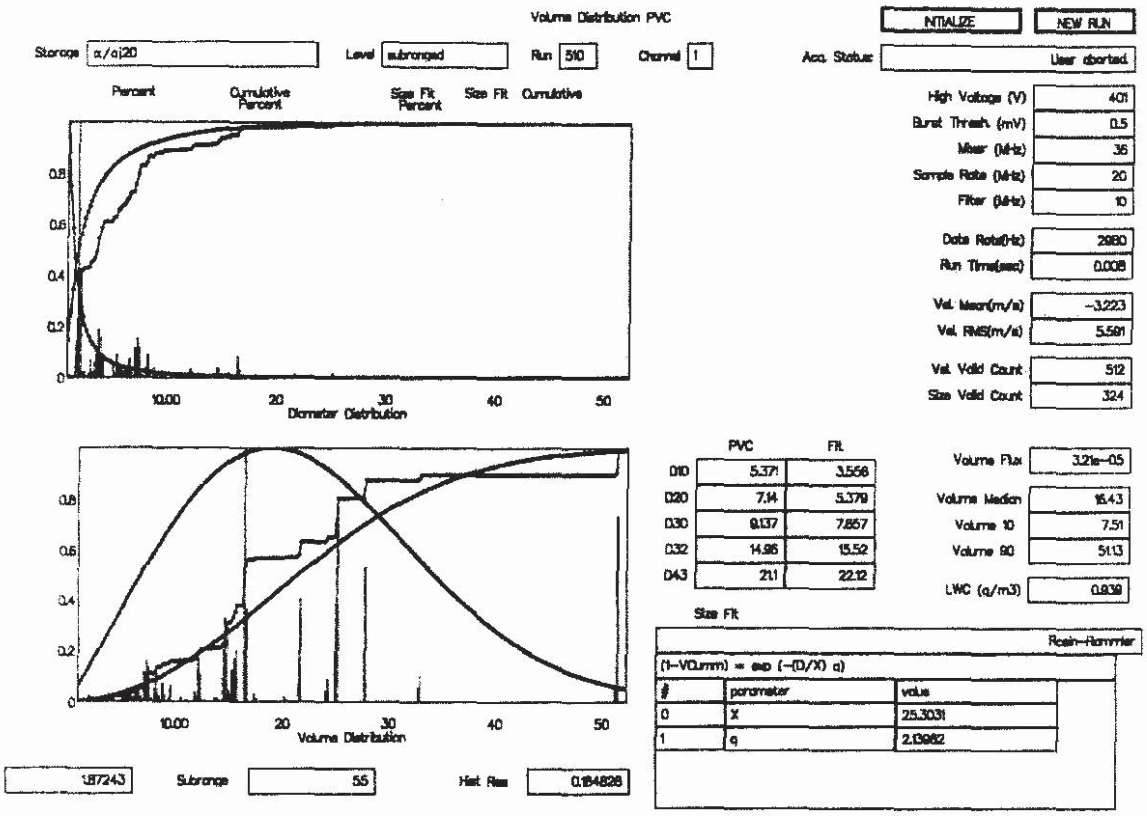


*Fig. 24. Cumulative size and volume distributions of droplets for novel experimental prototype injector with rotational - reciprocal movement of needle*

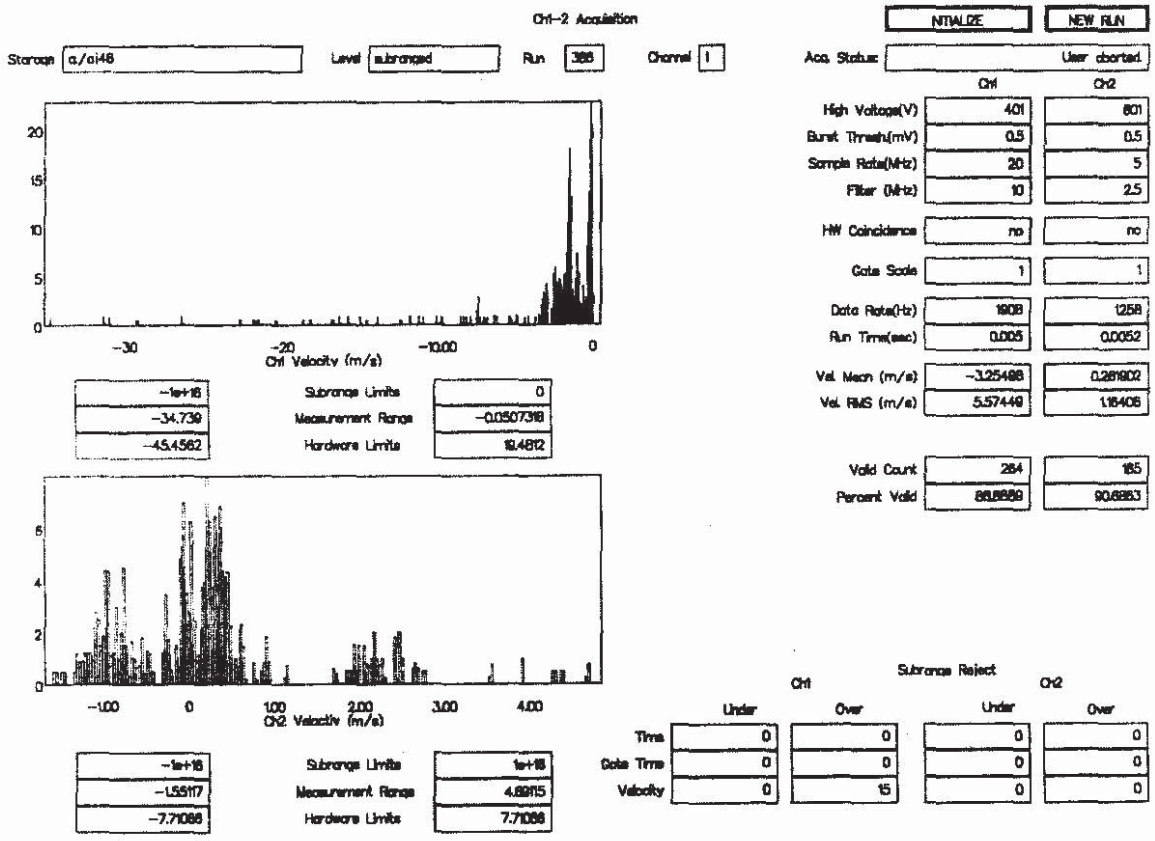


*Fig. 25. Velocity components of droplets for novel experimental prototype injector with rotational - reciprocal movement of needle after improvement (Ch1 and Ch2 – parallel and perpendicular to injector axis as appropriate*

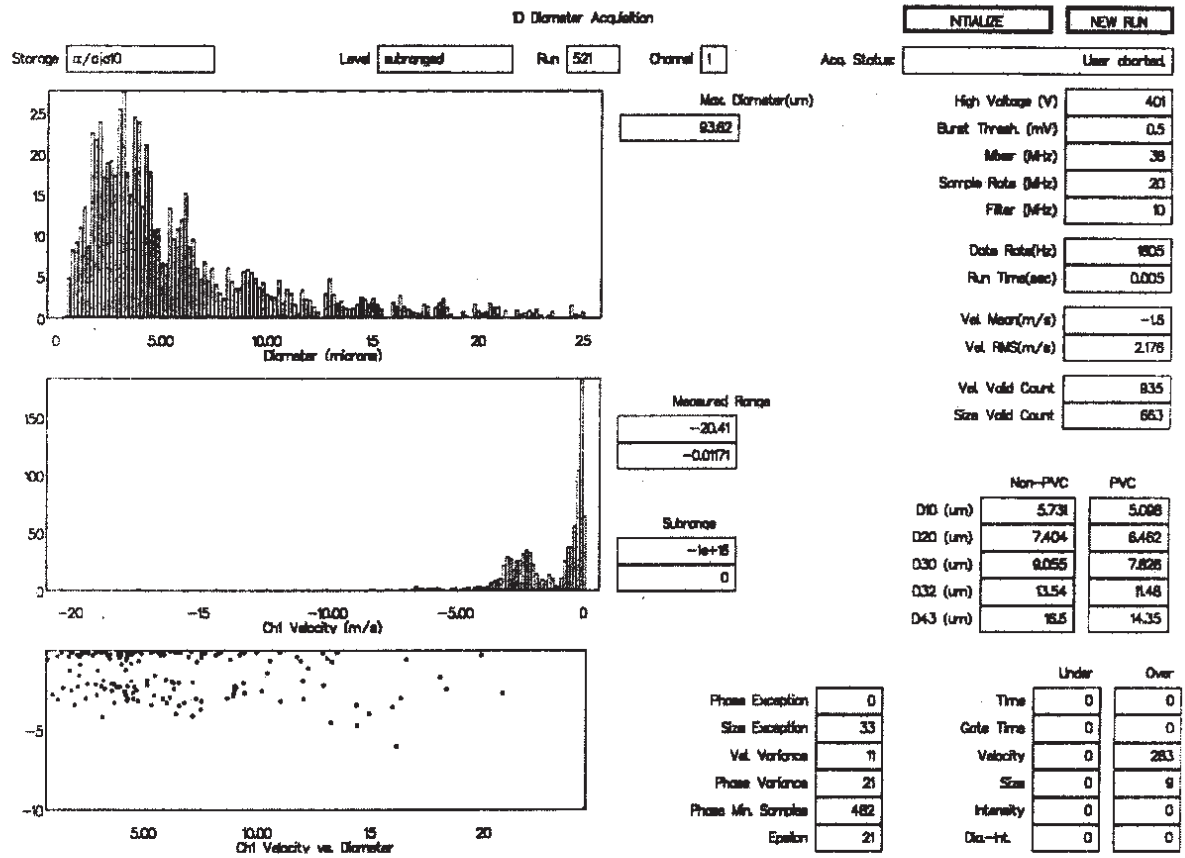


*Fig. 26. Mean diameters (D10, D20, D30, D32, D43) of droplets for novel experimental prototype injector with rotational - reciprocal movement of needle after improvement*

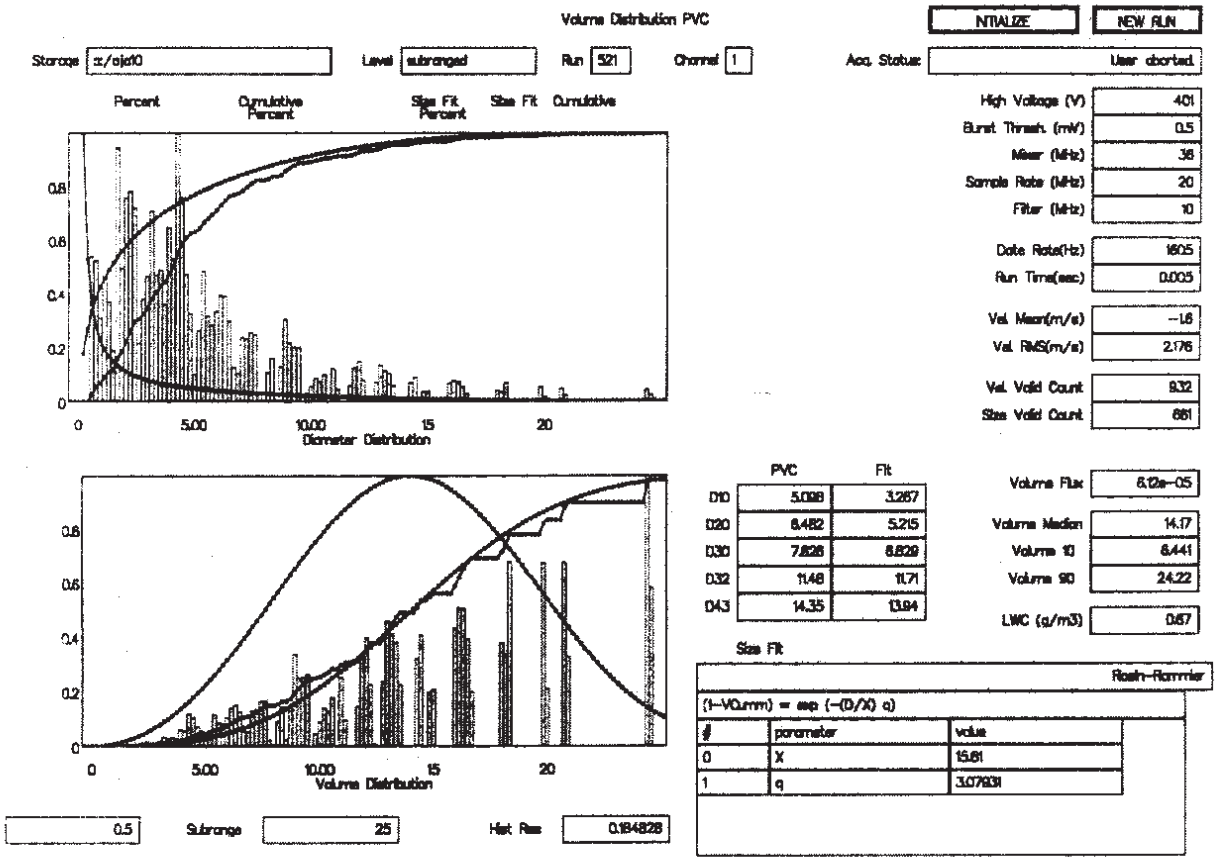


*Fig. 27. Cumulative size and volume distributions of droplets for novel experimental prototype injector with rotational - reciprocal movement of needle after improvement*

## 7. Summary

Novel experimental prototype injector with rotational - reciprocal movement of needle has some advantages, but experiments results were not as good as expected. Those were mainly because of prototype manufacturing but not only. Moreover orifice changes brought about negative effects during fuel flow closing. Time analysis of laser researches confirmed that large droplets in fuel spray are produced at the end of the injection. The aim of further research will be directed to orifice shape improvement. Laser methods, especially PDPA is a good means for novel injector refinement. Main advantages confirmed during engine tests are: CO and HC emission levels decreasing. Other engine performances will be possible for improvement after size of droplets homogenisation and mean sizes of fuel droplets decreasing as well establishing proper points for opening and closing fuel flow.

Research results presented in this paper have the introductory character. They proved the efficiency of novel injector from the mechanical point of view. Its design parameters require matching to shape of combustion chamber and air charge swirl quality in engine. The research results seem to show that approved principle of variation of atomizer outlet orifices sets possibilities for obtaining changes in combustion which can lead to limiting the exhaust emissions of Diesel engines.

Laser measurements indicated that after removing large droplets from fuel spray, novel injector characteristics may be as good as standard's injector or better what together with very good fuel spray shape are good prognosis for further works on improvement of fuel consumption, emissions and engine noise.

*The paper partially supported by Ministry of Science and Information Technology in grant number: 5T12D00924*

## References

[1] Gill D. W., Heimel G., Herzog P. L.: A Variable Nozzle Concept for High Speed DI Diesel Engines. IMechE Seminar on Diesel Fuel Injection Systems. 28-29 Sept 1995.

[2] Hasegawa T, Matsui K, Iwasaki T, Kobayashi T & Matsumoto Y.: Injection Characteristics and Spray Features of the Variable Orifice Nozzle (VON) for Direct Injection Diesel Engines. SAE 980807

[3] Jankowski A., Sandel A.: Influence of Fuel Quality on Mixture Preparation and Exhaust Emissions From Diesel Engines with Common Rail System. Journal of KONES Internal Combustion Engines 2003, Vol. 10, No. 3-4.

[4] Soteriou C., Andrews R., Smith M., Torres N., Sankhalpara S.: The Flow Patterns and Sprays of Variable Orifice Nozzle Geometries for Diesel Injection. SAE 2000-01-0943.

[5] Sowa K., Zablocki M., Szymanski J.: Some Properties of the New Multiorifice Injection Design with Variable Cross Section of Injecting Holes (in Polish). Proceedings of AUTOPROGRESS-KONMOT 2002 Conference. 28-30 May 2002. Vol. 2. Internal Combustion Engines.

[6] Sowa K., Zablocki M., Jankowski A., Sandel A.: Diesel engine researches with varied cross section nozzle of injector from point of view emission reduction and fuel consumption. Journal of KONES Internal Combustion Engines 2003. Vol. 10, No. 3-4.

[7] Sowa K., Zabłocki M., Jankowski A., Sandel A.: Investigations of varied cross section nozzle of injector of Diesel engine for performance improving and toxic exhaust gases emission reducing. The Archives of Automotive Engineering. Vol. 7. No. 3. 2004.

[8] Yarnamoto H., Nilmura K.: Characteristics of Fuel Sprays from Specially Shaped and Impinging Flow Nozzles. SAE 950082.

[9] Zabłocki M., Szymański J.: Wtryskiwacz paliwa do silnika spalinowego. Urząd Patentowy RP. P94889.